Available online at www.sciencedirect.com
SCIENCE DIRECT®
Scripta Materialia 51 (2004) 333–337
Scripta MATERIALIA
www.actamat-journals.com

Three dimensional atom probe investigation on the formation of $Al_3(Sc,Zr)$-dispersoids in aluminium alloys

B. Forbord [a,b], W. Lefebvre [c], F. Danoix [c,*], H. Hallem [a], K. Marthinsen [a]

[a] *Norwegian University of Science and Technology, 7491 Trondheim, Norway*
[b] *SINTEF Materials Technology, 7465 Trondheim, Norway*
[c] *Groupe de Physique des Matériaux, UMR CNRS 6634, University of Rouen, 76 801 Saint Etienne du Rouvray Cedex, France*

Received 22 March 2004; received in revised form 26 March 2004; accepted 29 March 2004
Available online 14 May 2004

Abstract

Three dimensional atom-probe (3DAP) has been applied in order to study the nucleation of small, spherical and coherent $Al_3(Sc,Zr)$-dispersoids. The results indicate that $Al_3(Sc,Zr)$ in the beginning of the nucleation process mainly consist of Al and Sc, while Zr enters the dispersoids at a later stage, i.e. relatively Zr-rich shells seem to form around Sc-rich cores.

Keywords: Aluminium alloys; Rare earth; Dispersoids; Nucleation; 3DAP

1. Introduction

Both Zr and Sc form dispersoids, which effectively inhibit recrystallisation and the corresponding strength loss during heat exposure of aluminium alloys. Recrystallisation involves the formation of strain-free nuclei/subgrains and the subsequent growth of these into the surrounding matrix. However, this will only occur if the subgrains are able to grow larger than a certain size, R_C, given by the Gibbs–Thomson relationship

$$R > R_C = \frac{4 \cdot \gamma_{GB}}{P_D - P_Z} \quad (1)$$

where R_C is the critical radius for nucleation, γ_{GB} is the specific grain boundary energy, P_D is the stored deformation energy and P_Z is the retarding force (Zener drag) that the dispersoids exert upon moving subgrain boundaries. Eq. (1) shows that when $P_Z \to P_D$ and $R_C \to \infty$ the structure is stabilised, i.e. recrystallisation is avoided. A widely used estimate for the Zener drag [1] is

$$P_Z = \frac{3 \cdot f \cdot \gamma_{GB}}{2 \cdot r} \quad (2)$$

where r is the radius and f is the volume fraction of dispersoids. Eq. (2) shows that a high Zener drag is obtained when the (f/r)-ratio is large. It is also important that the dispersoids precipitate quickly (in order to be present in the structure before recrystallisation begins), are thermally stable and are homogeneously distributed in order to maintain a high (f/r)-ratio everywhere in the structure even at high temperatures.

As both precipitation and coarsening are strongly linked to the diffusion rate of the dispersoid-forming element, it is easy to understand that it would be difficult to obtain both fast precipitation and high thermal stability by a single addition of for instance Sc. Sc diffuses relatively fast in Al [2,3] and the addition of this element leads to rapid and homogeneous nucleation of coherent and stable Al_3Sc-dispersoids (cubic $L1_2$-structure), but the high diffusivity of Sc also implies that these dispersoids may coarsen relatively fast. However, this has been solved by adding Sc in combination with Zr. Combined Sc/Zr-additions lead to the formation of $Al_3(Sc,Zr)$-dispersoids with very attractive properties, as they nucleate rapidly at high number densities, are homogeneously distributed and coarsen quite slowly [3–5]. Taking the fast precipitation kinetics of $Al_3(Sc,Zr)$ and the slow diffusion rate of Zr [3,6,7] into account, it seems to be a reasonable assumption that these dispersoids must be rich in Sc in the early stages of nucleation, i.e.

* Corresponding author. Tel.: +33-2-32-95-50-43; fax: +33-2-32-95-50-34.
E-mail address: frederic.danoix@univ-rouen.fr (F. Danoix).

1359-6462/$ - see front matter © 2004 Published by Elsevier Ltd. on behalf of Acta Materialia Inc.
doi:10.1016/j.scriptamat.2004.03.033

$Al_3(Sc,Zr)$ may initially form as Al_3Sc-phases. If this hypothesis is correct Zr enters the dispersoids at a later stage, possibly forming a more Zr-rich shell around the Sc-rich core. This work aims to investigate if there really is a relationship between the excellent properties of $Al_3(Sc,Zr)$ and the distribution of Zr and Sc within the dispersoid. AP-FIM (Atom Probe Field Ion Microscopy), which allows for the imaging of individual atoms in direct lattice space with a sub-nanometric resolution, has been applied for this task.

2. Alloy selection and preliminary experimental work

2.1. Casting

A ternary Al–Sc–Zr alloy was made by mixing appropriate amounts of Vigeland metal (99.99% Al) and master alloys of Al–10wt%Zr and Al–2wt%Sc, in order to produce an Al–0.08wt%Zr–0.15wt%Sc bulk. The alloy was directionally solidified in order to reduce porosity and solidification contraction at the top. A well stirred melt was poured at 760 °C into a cylindrical fibre tube mould ($\varnothing$ 40×150 mm) and cooled in the bottom by a large copper cylinder. The actual temperature was monitored by thermocouples during solidification, and the cooling rate was found to vary between 5–10 °C/s. No grain refiner was added during casting.

Precipitation annealing was carried out in a Heraeus K750 forced air circulation furnace. The alloy was annealed from room temperature to 475 °C by a 50 °C/h ramp and held at that temperature for 15 h in order to produce a dense distribution of dispersoids. The material was water-quenched after annealing.

An investigation using a Jeol 2010 TEM operated at 200 kV was carried out in order to study the dispersoid distribution after precipitation annealing. TEM-samples were prepared by electrothinning at 13 V in a Struers Tenupol. The electrolyte was a mixture of 75% methanol and 25% nitric acid and thinning was performed at −25 °C. Electron Energy Loss Spectroscopy (EELS) was used in order to measure the thickness of the TEM-foils, and the average dispersoid size, number density and volume fraction were subsequently determined from dark field images analysed by the computer programs Adobe Photoshop and ImageTool. Approximately 700 dispersoids were measured. Energy Dispersive Spectrometry (EDS) was used in order to investigate the chemical composition of the dispersoids. Several dispersoids, both in the proximity to and far away from boundaries, were investigated in order to study if the Sc- and Zr-content varied with position.

Three dimensional atom probe analyses were carried out on an Energy Compensated Optical Tomographic Atom Probe (ECOTAP [8]) developed in the University of Rouen. Details on the technique can be found elsewhere [9,10]. $0.3\times0.3\times20$ mm^3 blanks were cut from the $\varnothing$ 40 mm tubes, and prepared into needles by standard electropolishing in 2% perchloric acid (70%) in 2-butoxyethanol at 15 V at room temperature. Data analyses were conducted using the software developed in the University of Rouen.

3. Results and discussion

3.1. Precipitation annealing

TEM investigations indicate that the bulk material after casting is free of any Sc- or Zr-bearing phases, coarse or fine, and therefore can be considered as a supersaturated solid solution. Precipitation annealing (15 h annealing at 475 °C) resulted in a high density of small, coherent and homogeneously distributed $Al_3(Sc,Zr)$-phases, as shown in Fig. 1. EDS-analysis revealed that the dispersoids contained more Sc than Zr, regardless of whether they were far away from or in the proximity of boundaries, i.e. pure Al_3Sc or Al_3Zr-phases were not detected despite the fact that Zr and Sc segregate to grain/dendrite centres and grain boundaries during casting, respectively [11,12]. This result is in accordance with Riddle [13] and Costello [14], who have shown by microanalysis that all the dispersoids in their Sc/Zr-containing alloys were of the type $Al_3(Sc,Zr)$ regardless of their position. Furthermore, modelling predictions by Robson [15], on an alloy with a higher Zr/Sc-ratio than the present one, revealed that all dispersoids contained more Sc than Zr even in the dendrite centres.

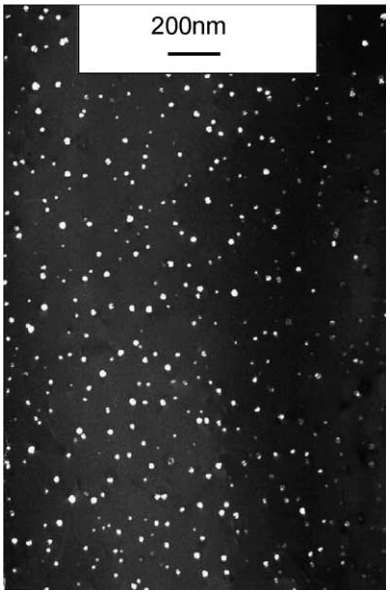

Fig. 1. Dark field TEM-micrograph showing the high density of homogeneously distributed $Al_3(Sc,Zr)$-dispersoids after precipitation annealing for 15 h at 475 °C.

Precipitation characteristics, as derived from TEM micrographs, are as follows: the dispersoid mean radius is 9.6 nm, their number density 2×10^{21} m^{-3} and the volume fraction 0.6%.

3.2. 3DAP analysis of the matrix

In order to study solute distribution in $Al_3(Sc,Zr)$-dispersoids, three dimensional atom probe analyses were conducted on the material annealed 15 h at 475 °C. The first step in data processing is the identification of the mass spectrum peaks to the chemical species according to their mass over charge ratios, as shown in Table 1.

As seen in this table, and according to the existing literature [9], there is a possible overlap between Sc and Zr at 45 amu. In order to quantify this overlap, the importance of each peak in the range 45–48.5 amu has been compared to the natural abundance of Zr isotopes. Results shown in Table 2 clearly indicate that the ratio of the isotopes from 45 to 48.5 amu is consistent with the natural abundance of the Zr isotopes, thus ruling out the presence of Sc^+ at 45 amu. As a consequence, all ions detected with a mass over charge ratio of 45 will be considered as Zr.

3.3. Internal morphology of $Al_3(Sc,Zr)$-dispersoids

A 3D atom probe analysis was conducted along a ⟨1 1 0⟩ axis in the aluminium, and several dispersoids were intercepted. The analysed volume has been reconstructed using the procedure described by Bas [16]. The (1 1 0) type planes are visible in the matrix, as shown in Fig. 2a. However, they do not appear in the dispersoids, whereas they should, according to the cube on cube orientation between the Al matrix and $Al_3(Sc,Zr)$-dispersoids [3]. Furthermore, the dispersoids appear as plate-like shaped disks, perpendicular to the analysis direction. This effect is a classical artifact of the reconstruction procedure, which does not account for the difference in evaporation fields between the matrix and the dispersoids, which has been shown to be significant in the case of Al matrix-Al_3Zr dispersoids [17].

Table 1
Definition of element intervals in the mass spectrum

Element	Possible charge (n)	m/n ratio (amu)
Al	1+: 2+: 3+	27:13.5:9
Sc	1+: 2+	45:22.5
Zr	1+: 2+: 3+	90–97:45–48.5:30–32.3

Table 2
Comparison between natural abundance and experimental proportions of Zr isotopes

Zr isotope (amu)	Natural abundance	Measured Zr^{2+}	Measured Zr^{3+}
90	51.45	47.5 ± 5	50.3 ± 8
91	11.22	9 ± 2	9.5 ± 3
92	17.15	19 ± 3	18 ± 5
94	17.38	20 ± 3	21 ± 5
96	2.8	4.5 ± 1.5	1.2 ± 1.2

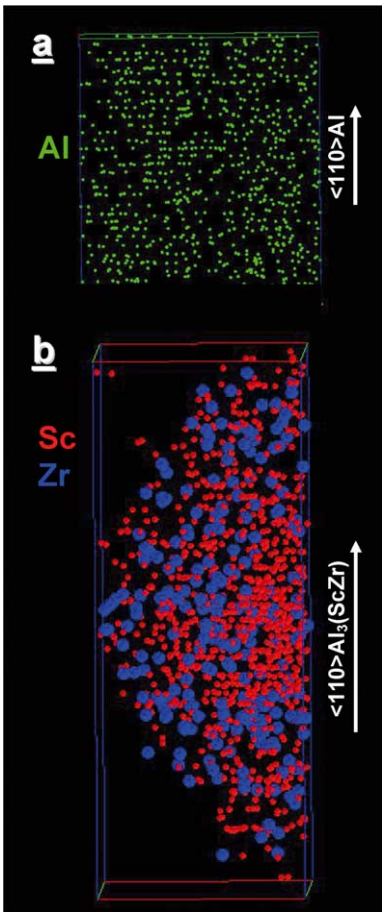

Fig. 2. (a) Aluminium (green dots) atom distribution within the matrix. The overall matrix volume represented is $4.5\times4.5\times5.5$ nm^3. (b) Solute distribution within a dispersoid—red dots are Sc atoms and blue dots Zr atoms. The overall represented volume is $6.6\times6.6\times17$ nm^3.

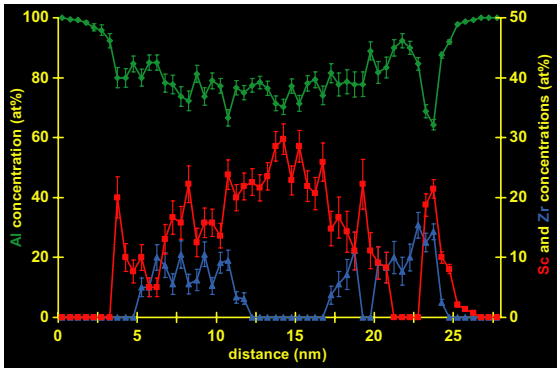

Fig. 3. Concentration profile through a $Al_3(Sc,Zr)$ precipitate.

Therefore, in order to get an accurate reconstruction of the dispersoids, a more appropriate value of the dispersoid evaporation field must be used.

An estimate of the difference in the evaporation fields between the matrix and the precipitates may be obtained by comparison of the state charge of Al ions in both phases [18]. When applied, this procedure leads to an evaporation field about 30% larger in the dispersoids (28–22 V/nm). With this correction applied, a new reconstruction was obtained, as shown in Fig. 2b. The Sc-rich (1 1 0) atomic planes in the centre of the dispersoid appear flat. In this region, 14 atomic planes containing Sc were counted, leading to an interplanar spacing of 0.29 nm, consistent with $d_{110}Al_3(Sc,Zr)$. Therefore, the reconstruction and the depth scaling are considered as satisfactory in the precipitate. It should be kept in mind that this corrected value can only be applied to the dispersoids, and should not be used for the matrix.

The limits of the precipitate itself have been determined by means of a cluster identification algorithm. The principle is as follows: around each atom in the analysed volume, the composition is measured in a spherical shell (1 nm in diameter in this case). If the local concentration is higher than a given threshold (set as (%Sc + %Zr)>5at% in this case), the atom is considered as belonging to the precipitate. The dispersoid's mean composition has been measured to 74 ± 0.5at%Al–21.5 ± 1at%Sc–4.5 ± 1at%Zr. This concentration perfectly matches with the $Al_3(Sc,Zr)$ stoichiometry, and with EDS analyses indicating that dispersoids are rich in Sc. Nevertheless, it is clear from Fig. 2b that Zr atoms are not homogeneously distributed within the dispersoid. Indeed, one can easily notice that the centre of the dispersoid looks Sc-rich whereas Zr ions are apparently situated closer to the matrix/dispersoid interface. In order to better show the local distribution of solute elements in the dispersoid, a concentration profile has been drawn across the precipitate (Fig. 3). This concentration profile clearly evidences that the dispersoid has a duplex morphology, consisting in a 5 nm diameter core, surrounded by a 8 nm thick shell. The core has an average Al_3Sc composition, whereas the shell incorporates most of the Zr atoms of the dispersoid. This result is in excellent agreement with the internal structure of $Al_3(Sc,Zr)$ proposed by Clouet [19] on the basis of Monte Carlo simulations. Also evidenced on this concentration profile, the diameter of this dispersoid (about 20 nm) is in good agreement with TEM observations.

3.4. Early stages of $Al_3(Sc,Zr)$-nucleation

The Sc-rich core strongly indicates that the dispersoid in the early stages of formation probably has consisted only of Al and Sc, i.e. due to the high diffusion rate of Sc compared to Zr in aluminium [2,6,7], the dispersoids can probably be regarded as Al_3Sc-phases early in the nucleation process. This observation most likely explains why $Al_3(Sc,Zr)$ and Al_3Sc display the same rapid precipitation kinetics.

3.5. The influence of Zr on the coarsening of $Al_3(Sc,Zr)$-dispersoids

The higher content of Zr in the outer layers of $Al_3(Sc,Zr)$, may be the reason for the lower coarsening rate of these dispersoids compared to Al_3Sc. If coarsening is controlled by diffusion, it is important that the rate controlling element diffuses as slowly as possible. Vetrano and Henager [20] studied the chemical composition of $Al_3(Sc,Zr)$ precipitates in an Al–4.45at%Mg–0.49at%Mn–0.18at%Sc–0.03at%Zr-alloy and detected Zr at the α-Al/$Al_3(Sc,Zr)$-interfaces. It was suggested that Zr acted as a barrier to Sc-diffusion across the interface, which in turn led to a reduction in the coarsening rate of Al_3Sc precipitates. This observation is in good accordance with the results obtained here. Furthermore, the interfacial energy, γ, should be minimised in order to obtain thermal stability [21]. It has been shown that the $Al_3(Sc,Zr)$/matrix lattice mismatch is smaller than the mismatch between Al_3Sc and matrix [22,23], and coherency can consequently be maintained to higher diameters for the former dispersoid type. As loss of coherency increases the interfacial energy, γ, and consequently also the rate of coarsening, this may also explain why $Al_3(Sc,Zr)$-dispersoids display a higher thermal stability than Al_3Sc.

4. Conclusions

The precipitation of $Al_3(Sc,Zr)$-dispersoids has been successfully studied by means of TEM and 3DAP. Dispersoids formed after 15 h at 475 °C are shown to be Sc-rich. Solute distribution in the dispersoids is heterogeneous, with a Sc-rich core and a Zr enriched outer shell. This work confirms the hypothesis of an intense initial precipitation of Al_3Sc nuclei, favoured by the fast Sc-diffusion rate in the initial solid solution, followed by later Zr segregation, causing a lowering of the coarsening rate.

Acknowledgements

Financial support from Hydro Aluminium, Elkem ASA, the Norwegian Research Council through the project "Heat Treatment Fundamentals" (Project No. 143877/213) and NTNU through the strategic research program "Materials" is gratefully acknowledged.

References

[1] Nes E, Ryum N, Hunderi O. Acta Met 1985;33:11.
[2] Fujikawa S-I. Defect Diffusion Forum 1997;143–147:115.
[3] Riddle YW. PhD thesis. Georgia Institute of Technology. 2000.
[4] Davydov VG, Elagin VI, Zakharov VV, Rostov TD. Met Sci Heat Treat 1996;38:347.
[5] Zakharov VV. Met Sci Heat Treat 1997;39:61.
[6] Mehrer H. In: Neumann G, editor. Diffusion in Solid Metals and Alloys, vol. 26. Springer Verlag; 1992. p. 151.
[7] Wagner C. Z Elektrochemie 1961;65:581.
[8] Bémont E, Bostel A, Bouet M, Da Costa G, Chambreland S, Deconihout B, et al. Ultramicroscopy 2003;95:231.
[9] Miller MK, Cerezo A, Hetherington MG, Smith GDW. Atom probe field ion microscopy. Oxford: Oxford University Press; 1996.
[10] Miller MK. Atom probe tomography: analysis at the atomic level. New York: Kluwer Academic; 2000.
[11] Riddle YW, Hallem H, Ryum N. Mater Sci Forum 2002;396–402:563.
[12] Forbord B. In: ICAA9, Brisbane, Australia. 2004.
[13] Riddle YW, Sanders TH. Mater Sci Forum 2000;331–337:799.
[14] Costello FA. PhD thesis. UMIST; 2003.
[15] Robson JD. Acta Mater [submitted for publication].
[16] Bas P, Bostel A, Deconihout B, Blavette D. Appl Surf Sci 8 1995;87–88(8):298.
[17] Cerezo A. Communication at Atom Probe Tomography Workshop, Oak Ridge National Laboratoty, TN, USA. 2003.
[18] Haydock R, Kingham DR. Phys Rev Lett 1980;44:1520.
[19] Clouet E. PhD thesis. Ecole Centrale de Paris. 2004.
[20] Vetrano JS, Henager CH. J Micros Micro 1999:160.
[21] Porter DA, Easterling KE. Phase transformations in metals and alloys. 3rd ed. Chapman and Hall; 1992. pp. 314–316.
[22] Harada Y, Dunand DC. Mater Sci Eng A 2002;329–331:686.
[23] Harada Y, Dunand DC. Sripta Mater 2003;48:219.